energies

MDPI

Article

Shielding Effectiveness Simulation of Small Perforated Shielding Enclosures Using FEM

Zdeněk Kubík * and Jiří Skála

Department of Applied Electronics and Telecommunications, University of West Bohemia, Pilsen 30614, Czech Republic; skalaj@kae.zcu.cz

* Correspondence: zdekubik@kae.zcu.cz; Tel.: +420-377-634-268

Academic Editor: Rodolfo Araneo

Received: 6 January 2016; Accepted: 18 February 2016; Published: 25 February 2016

Abstract: Numerical simulation of shielding effectiveness (SE) of a perforated shielding enclosure is carried out, using the finite element method (FEM). Possibilities of model definitions and differences between 2D and 3D models are discussed. An important part of any simulation is verification of the model results—here the simulation result are verified in terms of convergence of the model in dependence on the degrees of freedom (DOF) and by measurements. The experimental method is based on measurement of electric field inside the enclosure using an electric field probe with small dimensions is described in the paper. Solution of an illustrative example of SE by FEM is shown and simulation results are verified by experiments.

Keywords: electromagnetic compatibility (EMC); measurement; shielding effectiveness (SE); shielding enclosure; finite element method (FEM); simulation

1. Introduction

Nowadays, electronic devices contain a lot of highly energized parts, including processors, field-programmable gate arrays (FPGAs), power supplies and high-speed communications buses. But all these parts work on relatively low voltage levels and, therefore, they may often become victims of electromagnetic interference. One of its sources is high-speed data transmission. For these reasons, there exist many standards and recommendations concerning electromagnetically compatible environments. One part of electronic devices supporting a good level of EMC is electromagnetic shielding. Electromagnetic shielding mostly consists of shielding enclosures, gaskets, and ventilation structures. The shielding effectiveness (SE) is the term describing the quality of the shielding. There exist standards for SE measurement of shielding enclosures, but these standards do not respect the current trend—reduction of the device dimensions. For example, the IEEE standard for measuring the effectiveness of electromagnetic shielding enclosures [1] describes the measurement procedure for any enclosure having a smallest linear dimension greater or equal to 2.0 m. The question is, how to measure SE of such enclosures; the dimension of the measuring antenna depends on the wavelength and this antenna must be placed inside the shielding enclosures. If this is not possible, numerical or analytical methods can be used for determining SE. Analytical methods for SE calculation of the shielding enclosures with aperture are described in [2,3]. The numerical methods are well usable here, because it is easy to change geometry of the model. There are many suitable methods, including finite element method (FEM), method of moments (MoM), finite difference time domain method (FDTD) and others derived from them. Many papers can be found that deal with SE modelling—very interesting ones are [4–7]. This paper starts from previous articles [8–10] that are related to the problem of SE simulation.

1.1. Shielding effectiveness

The shielding effectiveness for electric and magnetic field is defined as the ratio (expressed in decibels) between the absolute value of electric field $\mathbf{E}_1$ (or magnetic field $\mathbf{H}_1$) at a point in space without the shielding and the absolute value of electric field $\mathbf{E}_2$ (or magnetic field $\mathbf{H}_2$) at the same point in space with the shielding [1]:

$$\mathrm{SE_E} = 20 \cdot \log \frac{|\mathbf{E}_1|}{|\mathbf{E}_2|} \ \ [\mathrm{dB}]\,, \tag{1}$$

$$\mathrm{SE_H} = 20 \cdot \log \frac{|\mathbf{H}_1|}{|\mathbf{H}_2|} \ \ [\mathrm{dB}] \tag{2}$$

These definitions are applicable for theoretical calculations and for situation where dimensions of the measuring antenna are negligible compared with the dimensions of the measured shielding enclosure. In real measurement cases, however, the measuring antenna does not have negligible dimensions and the measured values depend on the location of the antenna inside the enclosure. This problem is caused by the cavity resonances of the enclosure that decrease the SE.

Similar problems exist for simulations—there it is necessary to use the definition where the field is integrated through the whole cavity of the enclosure. The global shielding effectiveness (GSEs) for an electric/magnetic field is defined by [11]:

$$\mathrm{GSE_E} = 20 \cdot \log \frac{\int_V \mathbf{E}_1 \mathrm{d}V}{\int_V \mathbf{E}_2 \mathrm{d}V} \ \ [\mathrm{dB}]\,, \tag{3}$$

$$\mathrm{GSE_H} = 20 \cdot \log \frac{\int_V \mathbf{H}_1 \mathrm{d}V}{\int_V \mathbf{H}_2 \mathrm{d}V} \ \ [\mathrm{dB}] \tag{4}$$

Numerous factors decrease the SE of enclosures. There exist two most important factors: the first one is the cavity resonance of the box and the second one are the presence of apertures in the enclosure. The cavity resonance frequencies f_r are given by the formula [12]:

$$f_\mathrm{r} = \frac{1}{2\sqrt{\mu\varepsilon}} \sqrt{\left(\frac{m}{a}\right)^2 + \left(\frac{n}{b}\right)^2 + \left(\frac{p}{c}\right)^2} \ \ [\mathrm{Hz}] \tag{5}$$

where μ and ε represent the material parameters—permeability and permittivity of the cavity, a, b and c are the dimensions of the cavity (inside dimensions of the enclosure) and indexes m, n and p correspond to the resonance mode. The influence of the cavity resonances on SE is not easy to determine, because the influence of the field strength inside the cavity on the resonance depends on the quality factor Q of the resonator, which is often unknown.

Apertures in the enclosures have also a significant effect on the SE. The theoretical SE of a circular aperture with diameter r placed in a perfect shielding plate is [13]:

$$\mathrm{SE_{ap}} = 20 \cdot \log \frac{\lambda}{2\pi \cdot \mathrm{r}} \ \ [\mathrm{dB}] \tag{6}$$

and the SE for structure with n apertures (where the distance between apertures is less than a half-wavelength) is given by [13]:

$$\mathrm{SE_{n-ap}} = 20 \cdot \log \frac{\lambda}{2\pi \cdot \mathrm{r} \cdot \sqrt{n}} \ \ [\mathrm{dB}] \tag{7}$$

One of the ways for obtaining a high SE of the shielding enclosure is using cable glands, shielded air vent panels (honeycomb structures), and shielding gaskets.

1.2. Definitions of Numerical Models

The most important numerical methods for SE simulation are the finite element method, finite difference time domain method, method of moments, and their modifications. The general geometries of the models are similar for all these methods, but the definitions—initial and boundary conditions, distribution of mesh—could be different. The model consists of a free space surrounding the excitation source and geometry of the shielding enclosure (see Figure 1). Of course, from the definition of the SE, there is necessary to calculate two models—one with the enclosure and one without it (only with the observation area of the same dimensions as the internal dimension of the enclosure).

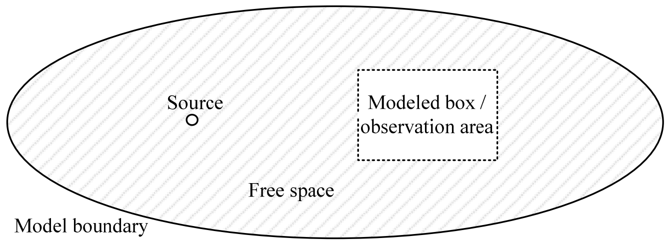

Figure 1. General description of SE model.

The setting of correct boundary conditions of the model is necessary for obtaining correct results. For example, the model boundary is usually modeled as a perfect magnetic ($\mathbf{n} \times \mathbf{H} = 0$) or electric ($\mathbf{n} \times \mathbf{E} = 0$) conductor, but a better choice is to use perfectly matched layer (PML), where the transition of the source signal is improved. The boundary of the box should be modeled as a perfect electric conductor (PEC), when the material of the box is made from a highly conducting material. The definition of the source depends on the method used, and for FEM it is possible to use a source of electric or magnetic field.

The SE simulations can be solved in two or three dimensions. For a 2D simulation, it is necessary to compute two models represented by two slices of the enclosure. Two sets of results from 2D simulations exhibit results comparable with a 3D simulation. The main difference is in the solution time, the 3D simulation requires much longer time. On the other side, 2D FEM models can be calculated by a solver with *hp*-adaptivity of the mesh, which provides very accurate results [8].

2. 3D Finite Element Method (FEM) Numerical Model

For finite element analysis in the frequency domain, the governing wave equation can be written as:

$$\nabla \times \frac{1}{\mu_r}(\nabla \times \mathbf{E}) = k_0^2 \left(\varepsilon_r - \frac{j\sigma}{\omega \varepsilon_0} \right) \mathbf{E} \tag{8}$$

where μ_r represents the relative permeability, ε_r stands for the relative permittivity, σ is electric conductivity, ε_0 represents the vacuum permittivity, and k_0 is the wave number of free space defined by the equation:

$$k_0 = \omega \sqrt{\varepsilon_0 \mu_0} = \frac{\omega}{c} \tag{9}$$

The source is modeled as an electric point dipole, the vector of electric current dipole moment being $\mathbf{P} = [0; 0; 1]\ \mathrm{m} \cdot \mathrm{A}$.

The shielding box is approximated by a PEC, where:

$$\mathbf{n} \times \mathbf{E} = 0 \tag{10}$$

For the analysis of fringing fields, a sphere of air was added around the model that is overlaid with a perfectly matched layer (PML). PML absorbs all radiated waves with small reflections by stretching the virtual domains into the complex plane using the following coordinate transform for the general space variable t:

$$t\prime = \left(\frac{t}{\Delta_{\mathrm{w}}}\right)^{n} (1 - i)\,\lambda F \qquad (11)$$

where Δ_{w} is the width of the PML region, n represents the PML order, λ is the frequency, and F denotes the scaling factor. The imaginary unit i satisfies the equation $i^2 = -1$.

3. Illustrative Example

A rectangular prism shielding enclosure was used for this illustrative example of SE simulation. Its dimensions are 291 mm × 277 mm × 243 mm and the thickness of its wall is 1 mm. The circular aperture of 10 mm diameter is placed in the center of the area 277 mm × 243 mm (see Figure 2a). The cavity dimensions are 289 mm × 275 mm × 241 mm.

Figure 2b represents a spherical area of the FEM model. There are visible four regions, the first of them representing the PMLs (on the model boundary) followed by a free space (surrounding enclosure). Inside the free space region there are placed the excitation source and shielding enclosure. The model represents the worst case; radiation from the source impacts the wall with the aperture. All parts were computed using Equations (8)–(11) by the software COMSOL Multiphysics.

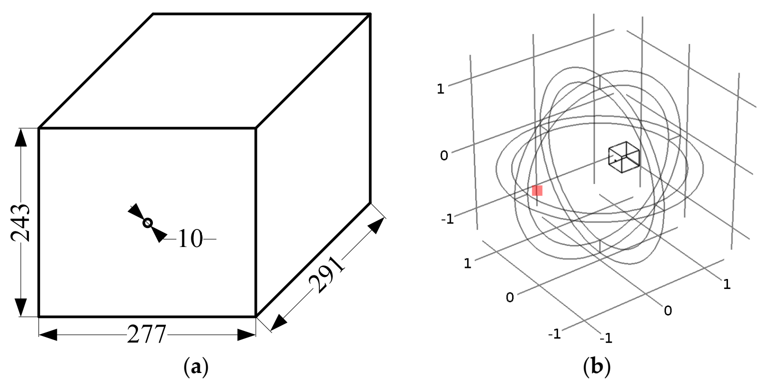

Figure 2. (**a**) Dimensions of shielding enclosure in millimeter; (**b**) area of the FEM model. The excitation source is placed at the red point, the enclosure is placed on the opposite side of the model. Here the dimensions are in m.

The FE mesh is shown in Figure 3. The size of the mesh was chosen with respect to the accuracy of the model—its important parts (shielding enclosure, free space area) were meshed more densely, while for PMLs we used sparser mesh. Five layers were used for modeling PMLs.

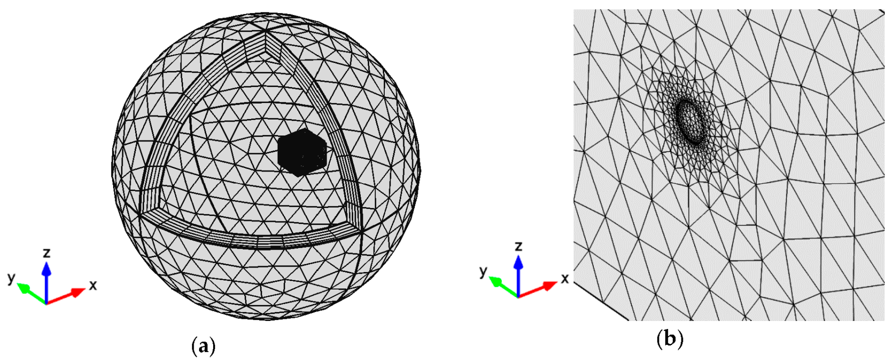

Figure 3. Distribution of the FE mesh. (**a**) FE mesh in the whole model. There are visible five layers of the PMLs, the black box inside the model represents a very fine FE mesh of the shielding enclosure; (**b**) detail of the FE mesh around the circular aperture of the enclosure.

The model was solved in the frequency domain. The simulation started at 500 MHz and ended at 2500 MHz. The frequency step—with respect to the computation time—was chosen 2.5 MHz. Overall, 800 simulation runs were carried out.

Important part of the simulation is verification of the result accuracy. Computing of the total electric energy inside the model is one possibility to check the solution accuracy:

$$\mathrm{w_e} = \frac{\mathrm{W_e}}{\mathrm{V}} \quad [\mathrm{J/m^3}] \tag{12}$$

where V represents the whole volume of the model and energy $\mathrm{W_e}$ is calculated from the expression:

$$\mathrm{W_e} = \int_V \frac{1}{2}\mathbf{ED}\,\mathrm{d}V = \int_V \frac{1}{2}\varepsilon_0 \mathbf{E}^2\,\mathrm{d}V \quad [\mathrm{J}] \tag{13}$$

The accuracy of the solution is good if the total electric energy does not change with the number of the degrees of freedom (DOFs). For the same number of DOFs, the accuracy will be better for lower frequencies; much more DOF must be used for high frequencies. Figure 4 shows the dependences of total electric energies on the number of DOFs of the model. There are three dependences corresponding to frequencies 500 MHz, 1500 MHz and 2500 MHz. The accuracy of the result at 500 MHz is obviously good. Different situation occurs with frequency 1500 MHz; the good accuracy of result begins at 1.15 million of DOFs. The worst situation is at frequency 2500 MHz—the total electric energy of the model is changing and the accuracy of the result cannot be guaranteed. A model with more DOF must be solved for high frequencies. The solution of such a model with a high number of DOF, however, requires longer calculation time and higher demands on hardware.

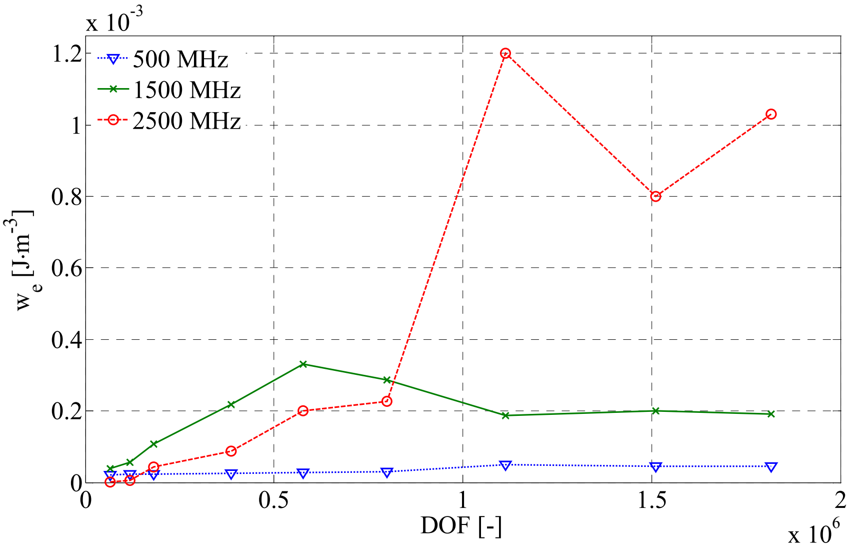

Figure 4. Total energy dependence on degree of freedom in the model with shielding enclosure. Example of the model convergence for frequencies 500 MHz, 1.5 GHz and 2.5 GHz.

Examples of simulation results are shown in Figures 5 and 6. These figures represent distributions of electric fields in the model at frequencies 752.5 MHz and 1172.5 MHz. The frequency 752.5 MHz responds to the lowest resonance mode of the cavity (theoretically at frequency 752.94 MHz). Figure 5 represents a sectional view of the model. There can be seen its slices in the *x*-*y* plane and *z*-*x* plane, respectively.

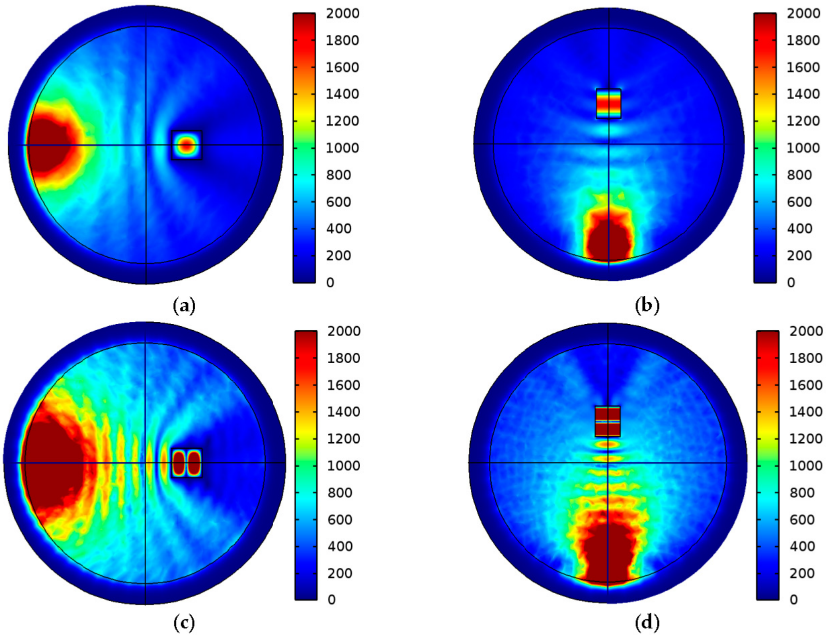

Figure 5. Distribution of the electric field E [V/m] in the model: (**a**) Frequency 752.5 MHz, *x*-*y* plane; (**b**) frequency 752.5 MHz, *z*-*x* plane; (**c**) frequency 1172.5 MHz, *x*-*y* plane; and (**d**) frequency 1172.5 MHz, *z*-*x* plane.

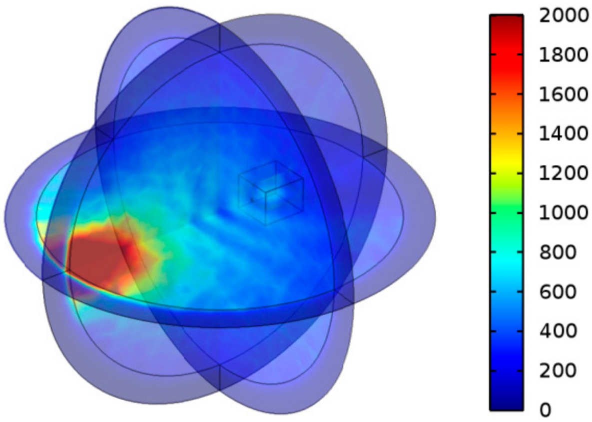

Figure 6. Distribution of electric field E [V/m] in the 3D model, frequency 752.5 MHz.

There are visible minima and maxima of electric field inside the cavity; if the field is changing in any direction, it responds to resonance mode 1 (or higher) in the same direction. One change from minimum to maximum and again back to minimum (or inverse) represents one index of the resonance mode. No change of electric field responds to zero resonance mode indexes. The first resonance mode TE110 is at the frequency 752.5 MHz, (*x*-*y*-*z* axes, dimensions 289 mm × 275 mm × 241 mm). A 3D view of the same solution is shown in Figure 6.

Figure 7 shows the dependence of simulated GSE on frequency and theoretical SE of circular aperture placed in ideally shielding plate that is calculated from Equation (6). There are visible influences of cavity resonances on SE—drops on the GSE trace, which represent decreases of GSE. Each drop responds to one TE resonance mode of the cavity. Of course, no drops of SE occur in the theoretical dependence.